

To the editorial office,

On behalf of all co-authors and myself, I hereby submit a revised version of our manuscript “Kinetic isotope effects in  $^{12}\text{CH}_3\text{D} + \text{OH}$  and  $^{13}\text{CH}_3\text{D} + \text{OH}$  from 278 to 313 K” (originally “Development of a new methane tracer: kinetic isotope effect of  $^{13}\text{CH}_3\text{D} + \text{OH}$  from 278 to 313 K”) We thank the three reviewers for carefully reading our manuscript and providing us with valuable feedback for improving the manuscript. We copy below the reviewer comments and a point-by-point response including all implemented changes to the original manuscript.

Sincerely,

Magnus Joelsson

**Reviewer 1:**

**1. Comment:** “Importance of isotope analysis for the atmospheric  $\text{CH}_4$  tracer? First of all, I do not agree with the title entitled ‘new atmospheric  $\text{CH}_4$  tracer’, and this is overselling of this experimental results. The title should be like ‘Kinetic isotope effect of  $^{13}\text{CH}_3\text{D} + \text{OH}$  from 278 to 313K’.”

**Response:** Title is changed to: “ Kinetic isotope effects in  $^{12}\text{CH}_3\text{D} + \text{OH}$  and  $^{13}\text{CH}_3\text{D} + \text{OH}$  from 278 to 313 K.”

**Comment:** “In current manuscript, authors explained a few about the importance for determination of isotopic fractionation in atmospheric methane sink reactions. Based on the previous studies using  $^{13}\text{C}$  and D, what do authors expect is main advantage of using clumped  $\text{CH}_4$  for better understanding of atmospheric methane cycles? In revised manuscript, following points should be addressed. (1) In the introduction, explain a bit more about how conventional isotopic information have helped understanding of atmospheric  $\text{CH}_4$  cycle. Describe the importance or possibility of the new  $\text{CH}_4$  tracer of clumped isotope well. How do authors aim to overcome the problems remained using clumped  $\text{CH}_4$ ? ”

**Response:** The following sentence is added to the Introduction: “Recent advances in mass spectrometry [1, 2] and laser infrared spectroscopy [3, 4] facilitate measurement of rare double-substituted isotopologues. The abundance of these “clumped” isotopologues (clumped refers to the rare isotopes being clumped together) generally follows a stochastic distribution (i.e.  $[^{12}\text{CH}_4][^{13}\text{CH}_3\text{D}] = [^{13}\text{CH}_4][^{12}\text{CH}_3\text{D}]$ ). However, small deviations from stochastic distribution can be induced by thermodynamic [5, 2, 6], kinetic [7, 4], and photolytic processes [8, 9]. Analysis of the clumped isotope anomaly in methane will yield unique constraints for the methane budget. Optical methods, as will be shown in this paper, provide high throughput and accuracy for overcoming the problems of analysis of clumped  $\text{CH}_4$ . The difference and advantage

of this approach is the additional information not available in single isotope analysis, especially regarding the mechanism of formation, independent of the enrichment of D and  $^{13}\text{C}$  in the starting material.” The following additional references is added in the introduction: “Thus, the construction of an accurate top-down methane budget by isotopic analysis, must take the isotopic signatures of both sources and sinks into account [10, 11, 12, 13].”

**Comment:** “What is the difference (and advantage) from conventional isotopic information of  $\text{CH}_4$ ?”

**Response:**  $\Delta(^{13}\text{CH}_3\text{D})$  offers an additional dimension in the isotopic fractionation space, furthermore a small  $\Delta(^{13}\text{CH}_3\text{D})$  in the sink would make the tracking of sources using  $\Delta(^{13}\text{CH}_3\text{D})$  more straight forward than conventional isotope fractionations. See response 2 below.

**Comment:** “(2) According to the results, not significant effects on clumped isotope were observed for  $\text{CH}_4 + \text{OH}$  reaction. For this case, readers might not understand the importance of atmospheric clumped  $\text{CH}_4$ . If authors suggest clumped  $\text{CH}_4$  is nice and new  $\text{CH}_4$  tracer in the title, I think this is an essential discussion for discussion section.”

**Response:** See response 2

2. **Comment:** “Atmospheric implication Authors should add section of ‘Atmospheric implication’ in discussion. If authors only present the experimental results, and brief discussion of the data, I do not think this paper is suitable for atmospheric chemistry journal like ACP. In revised manuscript, implication for the atmospheric chemistry should be discussed as much as author can. The determined isotopic fractionation for clumped isotope of  $\text{CH}_4$  enables us to discuss changes in isotopic composition of  $\text{CH}_4$  in the atmosphere. For example, if authors compare the results obtained in this study with other possible atmospheric reaction, which authors previously determined  $\text{CH}_4 + \text{Cl}$  reactions, authors would able to determine atmospheric fractionations. In addition, if expected changes in isotopic compositions for clumped isotope in the atmosphere are small for the sink reactions, the atmospheric clumped isotope of  $\text{CH}_4$  could still preserve the source information. This is nice and new tool to reconstruct source budget without any influences from sink reactions. Authors should add some interpretation and/or implication for atmosphere using investigated isotopic fractionation.”

**Response:** The “4.1 Atmospheric implication” section is added: “At steady state, assuming no clumping in emissions,  $\Delta(^{13}\text{CH}_3\text{D}) = \ln(\gamma)$ . It follows that  $\Delta(^{13}\text{CH}_3\text{D}) = 0.02 \pm 0.02$  implying that the clumped isotope effect of the OH reaction is very small. In turn, this implies that the bulk tropospheric  $\Delta(^{13}\text{CH}_3\text{D})$  reflects the source signal with relatively small adjustment due to the sink signal (i.e. mainly OH).  $\Delta(^{13}\text{CH}_3\text{D})$  would therefore be a more straightforward tracer for track-

ing methane sources than conventional isotopic analysis. However, the present uncertainty overrides the current estimated methane source signals [4], thus more precise measurements are necessary.”

3. **Comment:** “Data analysis is poorly described Authors explained very few for the data analysis and did not show raw data sets for the chamber experiments. First, as presented Figs S2-S4, the spectrum of measured, fitted and residuals should be presented in the main manuscript (not in the supporting information). If it is possible, the reference spectrum for CH<sub>4</sub> isotopologues and O<sub>3</sub> help reader’s understanding. Second, the spectrum fitting is one of the important possible errors in this relative rate plot method. Please explain well about the errors budget for each concentrations of CH<sub>4</sub> and its isotopologues for fitting calculation. For Fig S1, authors plotted the data without error bar for single calculation of MALT in current manuscript, but I think authors should add the error bar in all plots on the basis of calculation from MALT. I recommend to additional sub-section of data analysis for results, and then start discussion of isotope effect, and implication as I have already recommended.”

**Response:** Figures 1, 2, and 3 (attached) show the measured, key reference spectra, and the residual between the two for an example experiment. The error bars are included in the relative rate plots, but they are almost too small to see. The “2.4 Data analysis” sub-section is added. The following sentence is added in Sect. 2.4 to improve the description of the data analysis: “The experimental IR spectra were analyzed using the program MALT which simulates experimental FTIR spectra [14] combined with non-linear least squares fitting to best-fit the calculated spectra to measured spectra [15].”

4. **Comment:** “( $k(CH_4)/k(^{13}CH_4)$ )( $kCH_4/kCH_3D$ ) =  $k(CH_4)/k(^{13}CH_3D)$  is difficult to be understood, because no information for  $kCH_4/k^{13}CH_4$  were not presented. P27858 L1 The experimental section should be written in the past tense. This correction should be applied throughout this manuscript.”

**Response:** The sentence: “given the literature value of  $k(CH_4)/k(^{13}CH_4) = 1.0039 \pm 0.0002$ ” is added to the Abstract and the experimental part is changed to past tense.

## Reviewer 2:

1. **Comment:** “I find the title a bit misleading; consider removing the first part of the title.”

**Response:** Title is changed to: “Kinetic isotope effects in <sup>12</sup>CH<sub>3</sub>D + OH and <sup>13</sup>CH<sub>3</sub>D + OH from 278 to 313 K”

2. **Comment:** page 27854 lines 11–13: I think the phrase starting with ‘We find’ is not completely correct. The values mentioned here for the k ratios do not imply just by themselves that the CH<sub>4</sub> + OH KIE is multiplicative, but only when a value for  $k\text{CH}_4/k^{13}\text{CH}_4$  of about 1 is considered. Please consider changing the phrase to include this. The same comment for the similar phrase in Conclusions.”

**Response:** It is added that “ $k(\text{CH}_4)/k(^{13}\text{CH}_4) = 1.0039$ ” in the Conclusion and in the Abstract.

3. **Comment:** “Section 2.2 is called ‘Photoreactor’, but it only describes the reactor in the first paragraph; the rest of the subsection describes the actual experiments. I suggest splitting this subsection in two, such that the experiments are described separately.”

**Response:** The subsection “2.3 Laboratory procedure” is added to the manuscript

4. **Comment:** “page 27858 lines 16–17: ‘all at the concentrations given in Table 3’—I could not find the concentrations for all the listed species in Table 3, but only for O<sub>3</sub>. The text here could be corrected, but I actually think that it would be useful to give these (starting) concentrations in Table 3.”

**Response:** The methane, ozone, and water starting concentrations are now given in Table 1.

5. **Comment:** “In Sect 2.2 it is described how O<sub>3</sub> is produced and then photolyzed to O<sup>1</sup>D + O<sub>2</sub>, but the experiments should actually be on the CH<sub>4</sub> + OH reaction. Is it possible that some part went missing, the one that would describe how the OH is obtained and how the reaction with CH<sub>4</sub> takes place? Please add this information, in the current form it is not clear how the OH is obtained, and what the connection is between O<sub>3</sub> and the purpose of this paper.”

**Response:** Reaction (R7) “O(1D) +  $h\nu \rightarrow \text{OH} + \text{OH}$ ” is added.

6. **Comment:** “I suggest to include in the beginning of Sect 2 (before 2.1) or in the beginning of 2.2 a short overview of the experiments that have been done (one phrase) and already send to Table 3. In Sect 2.2 (page 27858 line 7) when the specifier ‘Experiments 1-4’ appears, the reader should already know that these exist.”

**Response:** A short experimental overview is added (Sect. 2): “Sixteen experiments were conducted, numbered from 1 through 16, see Table 1; eight (Experiments 1-8) for <sup>12</sup>CH<sub>3</sub>D and eight (Experiments 9-16) for <sup>13</sup>CH<sub>3</sub>D. The experiments were conducted at four different temperatures ( $T = [298, 278, 288, 313]\text{K} = [25, 5, 15, 40]^\circ\text{C}$ ); two experiments were conducted for each temperature.”

7. **Comment:** “I suggest that the tables should be reordered, with the one that is now Table 3 moved in front at ‘Table 1’”

**Response:** The Tables are ordered such that Table 1, 2, and 4 is now Table 3:5, Table 3 is split up in Table 1 and Table 2

8. **Comment:** “page 27858 lines 6–8: why were two detectors used?”

**Response:** The following sentence is added: “the MCT-detector is used in Experiments 1-4 for logistical reasons”

9. **Comment:** “page 27860 lines 2–4: I find this phrase unclear. If I understand correctly, the  $^{13}\text{CH}_3\text{D}$  is calculated from the 2140–2302 region, then the concentration calculated there is used to simulate the  $^{13}\text{CH}_3\text{D}$  spectrum in the 2850–3009 region, which is then used to correct the  $^{12}\text{CH}_4$  spectrum in the region 2850–3009, and from this the  $^{12}\text{CH}_4$  concentration. If my understanding is correct, please consider reformulating / clarifying the corresponding phrase in the paper.”

**Response:** The passage is changed to: “The concentrations of  $^{12}\text{CH}_3\text{D}$  and  $^{13}\text{CH}_3\text{D}$  were calculated from spectral fits in the region 2140–2302  $\text{cm}^{-1}$ , see Fig. 1 and 2. Interference from  $\text{H}_2\text{O}$ ,  $\text{CO}_2$ , and CO was eliminated by including simulated spectra obtained from the HITRAN database in the fit. As there is no HITRAN data available for  $^{13}\text{CH}_3\text{D}$  in this region, the cross sections from 2000–2400  $\text{cm}^{-1}$  for this isotologue were estimated by shifting the spectrum of  $^{12}\text{CH}_3\text{D}$ , see Joelsson et al. (2014). Concentrations of  $^{12}\text{CH}_4$  were calculated from spectral fits in the region 2838–2997  $\text{cm}^{-1}$ . Interference from  $^{13}\text{CH}_3\text{D}$  was reduced by including temperature adjusted reference spectra in the fit, and interference from  $^{12}\text{CH}_3\text{D}$ ,  $\text{H}_2\text{O}$ , and  $\text{H}_2\text{CO}$  was by including simulated spectra obtained from the HITRAN database in the fit, see Fig. 3. The spectral windows were sometimes adjusted to exclude saturated lines.”

10. **Comment:** “page 27860 line 15: unclear, how is the fitting method of York et al. adjusted?”

**Response:** The following sentence is added: “In the temperature dependence curve fitting procedure, the parameters  $A$  and  $B$  are from a linearized version of the Arrhenius equation: [...] are adjusted to match experimental. Also here, the method of York et al. (2004) was used.”

11. **Comment:** “page 27860 lines 16–20: I find this temperature description difficult to follow and I’m not sure I understand it correctly. Do you mean that, for each experiment, you take the average of the two sensors’ measurements over time, and the uncertainty is the stdev of all measurements? Please consider reformulating this part.”

**Response:** These lines are reformulated as: “The temperature in the cell was taken as the spatial average of the measurements from two

thermocouples inside the temperature housing. The experiment temperature was defined by the temporal mean of the spatially averaged temperature measurement series and the uncertainty of the experiment temperature was the standard deviation of the spatially averaged temperature measurement series.”

12. **Comment:** “page 27860, Sect. 2.4: please consider including an explanatory phrase in the beginning of this section, something like: ‘a kinetic model was used for …’ followed by the purpose of this exercise.”

**Response:** The following sentence is added in Sect. 2.5: A kinetic model was used to determine the influence of O(<sup>1</sup>D), reaction (R3), which rivals reaction (R1).

13. **Comment:** “page 27861, line 14: Please specify whether a correction for the reaction with O(<sup>1</sup>D) has been performed on the final CH<sub>4</sub> + OH results, or not.”

**Response:** The following sentence is added: “No correction is applied, and the possible deviation is included in the estimated error.”

14. **Comment:** “page 27861 lines 13- 14: the text here is unclear. The loss to O(<sup>1</sup>D) is estimated based on N<sub>2</sub>O at 2.3

**Response:** 4.7

15. **Comment:** “page 27863 line 10: the error for <sup>13</sup>C, D $\alpha$  is given as 0.01. Where is this coming from? If it is the stdev of the two values from experiments 9 and 10, then the number is not correct. Please verify and change if needed. Also, please adjust the error for D<sup>exp</sup> correspondingly.”

**Response:** This was a misprint: The uncertainty is 0.03 for  $k(\text{CH}_4)/k(^{13}\text{CH}_3\text{D})$

16. **Comment:** “I find the discussion and conclusion parts a bit too short. In particular, I think a discussion on the implications for the atmospheric CH<sub>4</sub> and for the possibility to use clumped isotopes to constrain its budget is missing. For example, would a non-existent or very small clumped isotope effect in the CH<sub>4</sub> + OH reaction, given that this is the main sink for CH<sub>4</sub>, improve the chances to follow the sources based on their clumped signatures? Please consider adding such a discussion, which would show the relevance of the results presented here for atmospheric CH<sub>4</sub>.”

**Response:** An Atmospheric implication section is added: “At steady state, assuming no clumping in emissions,  $\Delta(^{13}\text{CH}_3\text{D}) = \ln(\gamma)$ . It follows that  $\Delta(^{13}\text{CH}_3\text{D}) = 0.02 \pm 0.02$  implying that the clumped isotope effect of the OH reaction is very small. In turn, this implies that the

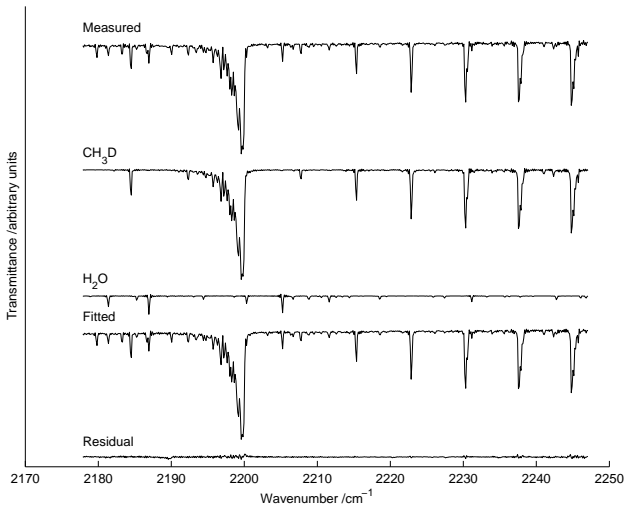


Figure 1: A typical spectral fit in the region where  $[^{12}\text{CH}_3\text{D}]$  is obtained (Experiment 5). Experimental data are shown by the topmost line, followed by the fitted (synthetic) partial spectra of the most dominant absorbers ( $\text{CH}_3\text{D}$  and  $\text{H}_2\text{O}$ ), the resulting fitted (synthetic) spectrum (also including  $\text{CO}_2$  and  $\text{CO}$ ), and the residual between the measured and fitted spectra is shown by the bottom line.

bulk tropospheric  $\Delta(^{13}\text{CH}_3\text{D})$  reflects the source signal with relatively small adjustment due to the sink signal (i.e. mainly OH).  $\Delta(^{13}\text{CH}_3\text{D})$  would therefore be a more straightforward tracer for tracking methane sources than conventional isotopic analysis. However, the present uncertainty overrides the current estimated methane source signals [4], thus more precise measurements are necessary.”

#### 17. Comment: Minor comments

**Response:** The manuscript should be change according to all minor comments

## References

- [1] Eiler et al., A high-resolution gas-source isotope ratio mass spectrometer, International Journal of Mass Spectrometry, 335, 45–56, 2013.
- [2] Stolper et al., Combined C-13-D and D-D clumping in methane: Methods and preliminary results, Geochimica Et Cosmochimica Acta, 126, 169–191, 2014.
- [3] Ono et al., Measurement of a Doubly Substituted Methane Isotopologue,  $^{13}\text{CH}_3\text{D}$ , by Tunable Infrared Laser Direct Absorption Spectroscopy, Analytical chemistry, 86, 13, 6487–6494, 2014.

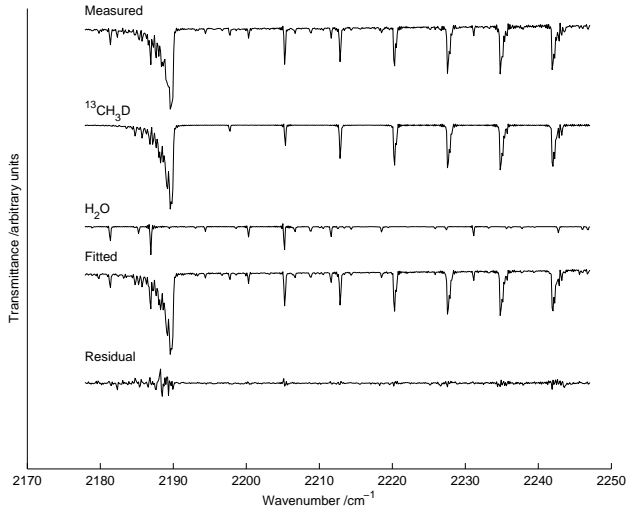


Figure 2: A typical spectral fit in the region where  $[^{13}\text{CH}_3\text{D}]$  is obtained (Experiment 10). Experimental data are shown by the topmost line, followed by the fitted (synthetic) partial spectra of the most dominant absorbers ( $^{13}\text{CH}_3\text{D}$  and  $\text{H}_2\text{O}$ ), the resulting fitted (synthetic) spectrum (also including  $\text{CO}_2$  and  $\text{CO}$ ), and the residual between the measured and fitted spectra is shown by the bottom line.

- [4] Wang et al., Nonequilibrium clumped isotope signals in microbial methane, *Science*, 348, 6233, 428–431, 2015.
- [5] Ma et al., Formation and abundance of doubly-substituted methane isotopologues (( $\text{CH}_3\text{D}$ ) – C – 13) in natural gas systems, *Geochimica et Cosmochimica Acta*, 72, 22, 5446–5456, 2008.
- [6] Liu and Liu, Clumped-isotope signatures at equilibrium of  $\text{CH}_4$ ,  $\text{NH}_3$ ,  $\text{H}_2\text{O}$ ,  $\text{H}_2\text{S}$  and  $\text{SO}_2$ , *Geochimica et Cosmochimica Acta*, 175, 252–270, 2016.
- [7] Joelsson et al., Relative rate study of the kinetic isotope effect in the ( $\text{CH}_3\text{D}$ ) – C – 13 + Cl reaction, *Chemical Physics Letters*, 605, 152–157, 2014.
- [8] Schmidt et al., Carbon dioxide photolysis from 150 to 210 nm: Singlet and triplet channel dynamics, UV-spectrum, and isotope effects, *Proceedings of the National Academy of Sciences*, 110, 44, 17691–17696, 2013.
- [9] Schmidt and Johnson, Clumped isotope perturbation in tropospheric nitrous oxide from stratospheric photolysis, *Geophysical Research Letters*, 42, 9, 3546–3552, 2015.
- [10] Quay, P. et al. The isotopic composition of atmospheric methane, *Global Biogeochemical Cycles*, 13, 2, 445–461, 1999.
- [11] Bergamaschi et al., Measurements of the carbon and hydrogen isotopes of atmospheric methane at Izaña, Tenerife: Seasonal cycles and synoptic-scale

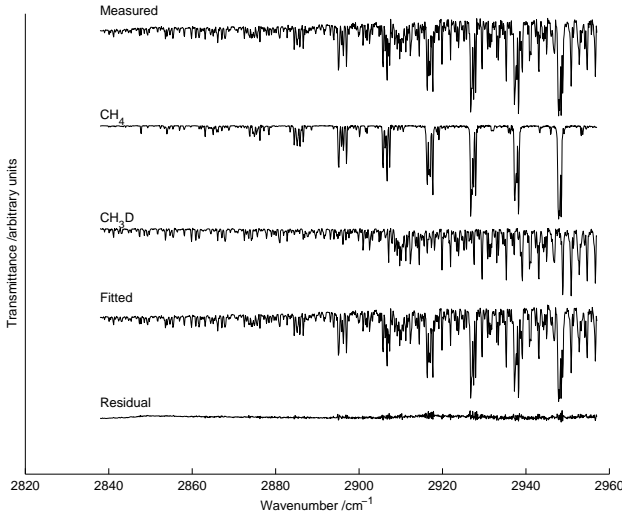


Figure 3: A typical spectral fit in the region where  $[^{12}\text{CH}_4]$  is obtained (Experiment 5). Experimental data are shown by the topmost line, followed by the fitted partial (synthetic) spectra of the most dominant absorbers ( $\text{CH}_4$  and  $\text{CH}_3\text{D}$ ), the resulting fitted (synthetic) spectrum (also including  $\text{H}_2\text{O}$ ), and the residual between the measured and fitted spectra is shown by the bottom line.

variations, Journal of Geophysical Research: Atmospheres, 105, D11, 14531–14546, 2000.

- [12] Allan et al., Active chlorine in the remote marine boundary layer: Modeling anomalous measurements of  $\delta^{13}\text{C}$  in methane, Geophysical research letters, 28, 17, 3239–3242, 2001.
- [13] Allan et al., Modeling the variation of  $\delta^{13}\text{C}$  in atmospheric methane: Phase ellipses and the kinetic isotope effect, Global biogeochemical cycles, 15, 2, 467–481, 2001.
- [14] Griffith, D. W. T., Synthetic Calibration and Quantitative Analysis of Gas-Phase FT-IR Spectra, Appl. Spectrosc., 50, 59–70, 1996.
- [15] Griffith et al., A Fourier transform infrared trace gas analyser for atmospheric applications, Atmospheric Measurement Techniques Discussions, 5, 3, 3717–3769, 2012.
- [16] York et al., Unified equations for the slope, intercept, and standard errors of best straight line, Am. J. Phys., 72, 3, 367–375, 2004.

Table 1: Experimental setup. The experiment numbers are listed in column Exp., the detector in the column Detect., the heavy CH<sub>4</sub> isotopologue included in the experiments are listed in column [<sup>x</sup>CH<sub>3</sub>D], the mean measured temperatures in the photoreactor are listed in column *T*, the H<sub>2</sub>O-vapour concentrations at the start of the experiments (*t* = 0) as obtain from spectral fitting are listed in column [H<sub>2</sub>O]<sub>*t*=0</sub>, the mean O<sub>3</sub> concentration after refill (i.e. the “top”-values) as obtain from spectral fitting are listed in column [O<sub>3</sub>]<sub>top</sub>, the <sup>12</sup>CH<sub>4</sub>-concentrations at the start of the experiments (*t* = 0) as obtain from spectral fitting are listed in column [<sup>12</sup>CH<sub>4</sub>]<sub>*t*=0</sub>, and the heavy CH<sub>4</sub> concentrations at the start of the experiments (*t* = 0) as obtain from spectral fitting are listed in column [<sup>x</sup>CH<sub>3</sub>D]<sub>*t*=0</sub>. Note that for the experiment including CH<sub>3</sub>D, the value of initial concentration only refers to [<sup>12</sup>CH<sub>3</sub>D]<sub>*t*=0</sub>.

Exp.	Detect.	<sup>x</sup> CH <sub>3</sub> D	<i>T</i>	[H <sub>2</sub> O] <sub><i>t</i>=0</sub>	[O <sub>3</sub> ] <sub>top</sub>	[ <sup>12</sup> CH <sub>4</sub> ] <sub><i>t</i>=0</sub>	[ <sup>x</sup> CH <sub>3</sub> D] <sub><i>t</i>=0</sub>
			K	hPa	hPa	hPa	hPa
1	MCT	CH <sub>3</sub> D	298.2 ± 1.2	7.1	— <sup>a</sup>	0.030	0.054
2	MCT	CH <sub>3</sub> D	297.6 ± 0.8	5.6	0.19	0.058	0.042
3	MCT	CH <sub>3</sub> D	277.2 ± 0.2	5.2	0.29	0.109	0.046
4	MCT	CH <sub>3</sub> D	277.0 ± 0.2	5.1	0.16	0.073	0.035
5	InSb	CH <sub>3</sub> D	284.5 ± 0.1	7.2	0.26	0.025	0.033
6	InSb	CH <sub>3</sub> D	291.1 ± 0.2	7.4	— <sup>a</sup>	0.052	0.050
7	InSb	CH <sub>3</sub> D	313.5 ± 1.3	7.1	0.17	0.025	0.029
8	InSb	CH <sub>3</sub> D	312.4 ± 0.9	4.3	— <sup>a</sup>	0.022	0.040
9	InSb	<sup>13</sup> CH <sub>3</sub> D	298.5 ± 0.1	5.1	— <sup>a</sup>	0.035	0.026
10	InSb	<sup>13</sup> CH <sub>3</sub> D	297.6 ± 0.6	6.4	0.13	0.025	0.033
11	InSb	<sup>13</sup> CH <sub>3</sub> D	276.8 ± 0.8	5.4	— <sup>a</sup>	0.024	0.024
12	InSb	<sup>13</sup> CH <sub>3</sub> D	277.2 ± 1.3	5.1	— <sup>a</sup>	0.022	0.030
13	InSb	<sup>13</sup> CH <sub>3</sub> D	287.4 ± 1.2	5.4	— <sup>a</sup>	0.021	0.028
14	InSb	<sup>13</sup> CH <sub>3</sub> D	287.4 ± 0.4	4.5	— <sup>a</sup>	0.016	0.029
15	InSb	<sup>13</sup> CH <sub>3</sub> D	314.4 ± 1.0	5.2	0.26	0.023	0.037
16	InSb	<sup>13</sup> CH <sub>3</sub> D	313.8 ± 0.8	8.3	0.17	0.025	0.035

<sup>a</sup>Spectra recorded during or after photolysis, [O<sub>3</sub>]<sub>top</sub> not available

# Kinetic isotope effects of $^{12}\text{CH}_3\text{D} + \text{OH}$ and $^{13}\text{CH}_3\text{D} + \text{OH}$ from 278 to 313 K

L. M. T. Joelsson<sup>1,3</sup>, J. A. Schmidt<sup>1</sup>, E. J. K. Nilsson<sup>2</sup>, T. Blunier<sup>3</sup>, D. W. T. Griffith<sup>4</sup>, S. Ono<sup>5</sup>, and M. S. Johnson<sup>1</sup>

<sup>1</sup>Department of Chemistry, University of Copenhagen, Copenhagen, Denmark

<sup>2</sup>Division of Combustion Physics, Department of Physics, Lund University, Sweden

<sup>3</sup>Centre for Ice and Climate (CIC), Niels Bohr Institute, University of Copenhagen, Copenhagen, Denmark

<sup>4</sup>University of Wollongong, Department of Chemistry, Wollongong, Australia

<sup>5</sup>Department of Earth, Atmospheric and Planetary Sciences, Massachusetts Institute of Technology, Cambridge, MA, USA

*Correspondence to:* M. S. Johnson (msj@kiku.dk)

**Abstract.** Methane is the second most important long lived greenhouse gas and plays a central role in the chemistry of the Earth's atmosphere. Nonetheless there are significant uncertainties in its source budget. Analysis of the isotopic composition of atmospheric methane, including doubly substituted species (e.g.  $^{13}\text{CH}_3\text{D}$ ), offers new constraints on the methane budget as the sources and sinks have distinct isotopic signatures. The most important sink of atmospheric methane is oxidation by OH in the troposphere which accounts for around 84 % of all methane removal. Here we present experimentally derived methane + OH kinetic isotope effects and their temperature dependence over the range of 278 to 313 K for  $\text{CH}_3\text{D}$  and  $^{13}\text{CH}_3\text{D}$ ; the latter is reported here for the first time. We find  $k_{\text{CH}_4}/k_{\text{CH}_3\text{D}} = 1.31 \pm 0.01$  and  $k_{\text{CH}_4}/k_{^{13}\text{CH}_3\text{D}} = 1.34 \pm 0.03$  at room temperature, implying that the methane + OH kinetic isotope effect is multiplicative such that  $(k_{\text{CH}_4}/k_{^{13}\text{CH}_4})(k_{\text{CH}_4}/k_{\text{CH}_3\text{D}}) = k_{\text{CH}_4}/k_{^{13}\text{CH}_3\text{D}}$ , within the experimental uncertainty, given the literature value of  $k_{\text{CH}_4}/k_{^{13}\text{CH}_4} = 1.0039 \pm 0.0002$ . In addition, the kinetic isotope effects were characterized using transition state theory with tunneling corrections. Good agreement between the experimental, quantum chemical, and available literature values was obtained. The theoretical calculation confirms that the  $^{13}\text{CH}_3\text{D}$  isotope effect is the product of D- and  $^{13}\text{C}$ - isotope effects. Based on the results we conclude that the OH reaction (the main sink of methane) at steady-state can produce an atmospheric clumped isotope signal ( $\Delta(^{13}\text{CH}_3\text{D}) = \ln([{\text{CH}_4}]^{^{13}\text{CH}_3\text{D}}/[^{13}\text{CH}_4][\text{CH}_3\text{D}])$ ) of  $0.02 \pm 0.02$ .

## 1 Introduction

Atmospheric methane is the subject of increasing interest from both the climate research community and the public due its impacts on climate change, as reported by the IPCC (2013). The direct radiative forcing of methane is  $0.64 \text{ Wm}^{-2}$ . Including feedback mechanisms and secondary effects e.g. increased  $\text{O}_3$  production, stratospheric water vapor and production of  $\text{CO}_2$ , methane's radiative forcing becomes  $0.97 \text{ Wm}^{-2}$ ,  $2/3$  of the forcing by  $\text{CO}_2$  over the same time period (IPCC, 2013, Fig. 8.15).

Atmospheric methane has both natural and anthropogenic sources and the two categories contribute about equally (Ciais et al., 2013, and references therein). Wetlands are the dominant natural source, and agriculture and waste are the largest anthropogenic sources. Fossil fuels make smaller contributions. A majority (84%) of atmospheric methane is removed by oxidation by OH in the troposphere:



oxidation in the troposphere by Cl contributes about 4% of the total:



About 8% of methane is removed in the stratosphere by radical oxidation, such as reactions (R2) and (R3):



The rest (4%) is removed by soil (Kirschke et al., 2013).

Carbon and hydrogen isotopic analysis are widely used to distinguish microbial and thermal sources of atmospheric methane (e.g., Lowe et al., 1997; Ferretti et al., 2005; Tyler et al., 2007; Lassey et al., 2007). However, reactions (R1), (R2), and (R3) produce relatively large D/H isotope effects (Saueressig et al., 1995, 1996, 2001; Crowley et al., 1999; Feilberg et al., 2005). Thus, the construction of an accurate top-down methane budget by isotopic analysis, must take the isotopic signatures of both sources and sinks into account (Quay et al., 1999; Bergamaschi et al., 2000; Allan et al., 2001a, b) [new references]. An isotope budget based on methane source (and sink) fractionations result in an underdetermined systems (e.g., Pohlman et al., 2009). Recent advances in mass spectrometry (Eiler et al., 2013; Stolper et al., 2014) and laser infrared spectroscopy (Ono et al., 2014; Wang et al., 2015) facilitate measurement of rare double-substituted isotopologues. The abundance of these “clumped” isotopologues (clumped refers to the rare isotopes being clumped together) generally follows a stochastic distribution (i.e.  $[{}^{12}\text{CH}_4][{}^{13}\text{CH}_3\text{D}] = [{}^{13}\text{CH}_4][{}^{12}\text{CH}_3\text{D}]$ ). However, small deviations from stochastic distribution can be induced by thermodynamic (Ma et al., 2008; Stolper et al., 2014; Liu and Liu, 2016), kinetic (Joelsson et al., 2014; Wang et al., 2015), and photolytic processes (Schmidt et al., 2013; Schmidt and Johnson, 2015). Analysis of the clumped

isotope anomaly in methane will yield unique constraints for the methane budget. Optical methods, as will be shown in this paper, provide high throughput and accuracy for overcoming the problems  
55 of analysis of clumped CH<sub>4</sub>. The difference and advantage of this approach is the additional information not available in single isotope analysis, especially regarding the mechanism of formation, independent of the enrichment of D and <sup>13</sup>C in the starting material.

The kinetic isotope effect <sup>j</sup>Eα is a characteristic property of each process:

$${}^j_E\alpha \equiv \frac{k({}^iE + OH)}{k({}^jE + OH)}, \quad (1)$$

60 where <sup>i</sup>E is the most abundant (here, the lighter) isotopologue, <sup>j</sup>E the rare (heavy) isotopologue, k(E + OH) is the reaction rate coefficient for the reaction E + OH. As a measure of how much of a fractionation of <sup>13</sup>CH<sub>3</sub>D kinetic reactions produce, the apparent clumpiness, γ is used. It is a measure of the effect of the clumped substitution on the reaction rate, as opposed to the combined effect of two single substitutions. It is defined as (Wang et al., 2015):

$$65 \quad \gamma \equiv \frac{{}^{13}C,D\alpha}{{}^{13}C\alpha \times {}^D\alpha} \quad (2)$$

A related measure is the Δ(<sup>13</sup>CH<sub>3</sub>D) value that quantifies the extent to which rare isotopes clump together to form a multiply substituted species, as opposed to a stochastic distribution (Ono et al., 2014):

$$\Delta({}^{13}\text{CH}_3\text{D}) \equiv \ln \left( \frac{[{}^{13}\text{CH}_3\text{D}][{}^{12}\text{CH}_4]}{[{}^{12}\text{CH}_3\text{D}][{}^{13}\text{CH}_4]} \right), \quad (3)$$

70 where [<sup>13</sup>CH<sub>3</sub>D], [<sup>12</sup>CH<sub>4</sub>], [<sup>12</sup>CH<sub>3</sub>D] and [<sup>13</sup>CH<sub>4</sub>] represent the concentrations of the different isotopologues.

The kinetic isotope effects for the singly substituted species CH<sub>3</sub>D and <sup>13</sup>CH<sub>4</sub> have been studied previously both experimentally and theoretically, see Tables 3 and 4 [table reordered] respectively. The kinetic isotope effect <sup>13</sup>C,Dα for the reaction with OH is not described in the existing literature.  
75 The related kinetic isotope effect for the CH<sub>4</sub> + Cl reaction was measured at room temperature with the present setup by Joelsson et al. (2014) and found to be 1.60 ± 0.04.

In the present study the kinetic isotope effects <sup>D</sup>α and <sup>13</sup>C,Dα are determined using the relative rate method. Species concentrations in the reaction cell are determined using Fourier Transform Infrared (FTIR) spectroscopy. Further, <sup>D</sup>α, <sup>13</sup>Cα, and <sup>13</sup>C,Dα are calculated using quantum chemistry and  
80 transition state theory.

## 2 Experimental procedures

Sixteen experiments were conducted, numbered from 1 through 16, see Table 1; eight (Experiments 1–8) for <sup>12</sup>CH<sub>3</sub>D and eight (Experiments 9–16) for <sup>13</sup>CH<sub>3</sub>D. The experiments were conducted at

85 four different temperatures ( $T = [298, 278, 288, 313]\text{K} = [25, 5, 15, 40]^\circ\text{C}$ ); two experiments were conducted for each temperature.

## 2.1 Relative rate method

The experiments were carried out using the relative rate method on a semi-static gas mixture. The decaying concentrations of reactants were measured as a function of the extent of reaction. Considering two bimolecular reactions with second order rate coefficients  $k_A$  and  $k_B$ ,



and assuming there were no other loss processes, the following relation holds:

$$\ln\left(\frac{[\text{A}]_0}{[\text{A}]_t}\right) = \frac{k_A}{k_B} \ln\left(\frac{[\text{B}]_0}{[\text{B}]_t}\right). \quad (4)$$

Here  $[\text{A}]_0$ ,  $[\text{A}]_t$ ,  $[\text{B}]_0$  and  $[\text{B}]_t$  represent the concentrations of compounds A and B at times 0 and  $t$  respectively. The slope of  $\ln([\text{A}]_0/[\text{A}]_t)$  versus  $\ln([\text{B}]_0/[\text{B}]_t)$  gives the relative reaction rate coefficient. In these experiments A is  $^{12}\text{CH}_4$  and B is  $^{12}\text{CH}_3\text{D}$  or  $^{13}\text{CH}_3\text{D}$ .

## 2.2 Photoreactor

Experiments were carried out in the photochemical reactor at the University of Copenhagen, Department of Chemistry. The reactor has been described in detail elsewhere (Nilsson et al., 2009). It consists of a 100 L quartz cell with multi-pass optics surrounded by 16 UV-C fluorescent Hg lamps in a temperature controlled housing. The cell is coupled to a Bruker IFS 66v/S FTIR spectrometer with either a mercury cadmium telluride (MCT) detector (Experiments 1–4) or an indium antimonide (InSb) (Experiments 5–16). The InSb-detector has a better signal-to-noise ratio, the MCT-detector is used in Experiments 1–4 for logistical reasons. Two thermocouple gauges are placed inside the temperature controlled housing to monitor the temperature and a pressure gauge is connected to the cell to monitor pressure inside the cell. The temperatures and the pressures were logged every 0.5 s.

## 2.3 Laboratory procedure

Gas mixes were prepared by expanding  $\text{H}_2\text{O}$  vapor (Milli-Q Ultrapure Water) into the chamber through a glass gas manifold. The two methane isotopologues  $\text{CH}_3\text{D}$  (Experiments 1–8) (purity > 98%, Cambridge Isotope Laboratories, Inc.) or  $^{13}\text{CH}_3\text{D}$  (Experiments 9–16), and  $\text{CH}_4$  (purity > 99%, Aldrich) and  $\text{O}_3$  were flushed into the chamber with a  $\text{N}_2$  buffer (purity 99.998%, Air Liquide), all at the concentrations given in Table 1 [table reordered].  $^{13}\text{CH}_3\text{D}$  was synthesized using the

Grignard reaction, see Joelsson et al. (2014). O<sub>3</sub> was generated from O<sub>2</sub> (purity 99.97 %, Air Liquide) using an ozone generator (Model AC-20, O<sub>3</sub> Technology), preconcentrated before injection on  
115 silica gel cooled with ethanol and dry ice to -67°C. The desired pressure in the cell (450 hPa) was obtained using N<sub>2</sub> as bath gas. The starting pressure is chosen such that the pressure is high enough for the N<sub>2</sub> to quench O(<sup>1</sup>D) radicals, but low enough to keep the final pressure below atmospheric pressure. The gas mixture was left to rest for up to 1.5 hours while several IR spectra were recorded to ensure that no instability or dark chemistry occurs in the gas mix. The UV-C lamps were lit for up  
120 to 5 min photolysing at least 75 % of the O<sub>3</sub> according to:



O(<sup>1</sup>D) then subsequently reacts with H<sub>2</sub>O to yield OH:



Up to 0.2 Pa O<sub>3</sub> was flushed with about 20 hPa N<sub>2</sub> into the chamber to compensate for the loss of  
125 ozone with time, mainly due to O(<sup>3</sup>P) + O<sub>3</sub>. A pressure gradient was established and maintained throughout the filling process such that no gas leaked back from the chamber into the gasline. Spectra were recorded at each filling step. The procedure was repeated until the mix had a final pressure of 933 hPa. Two experiments were conducted at each of the temperatures 278, 288, 298, and 313 K for each of the two heavy methane isotopologues. Exact temperatures are listed in Table 1 [new table].  
130 After each experiment a dilution test was performed: 133 hPa was pumped out and the chamber is refilled with 133 hPa N<sub>2</sub>. This was repeated 5–6 times. Ideally, concentration calculations from the spectral fits (data analysis described below) of the resulting spectra should give a linear fit with the slope of 1. The slope of these dilution tests are presented in Table 2 [new table]. In an extra experiment with <sup>12</sup>CH<sub>3</sub>D, N<sub>2</sub>O (Air Liquide, no purity information available) was added as an O(<sup>1</sup>D)  
135 tracer. The results from this experiment are used as a benchmark to validate a model that was constructed to investigate the extent of O(<sup>1</sup>D) chemistry, see Sect. 2.5. An example of an experimental plot can be found in Fig. 4 [new figure] and the full data set in Figs. S1–S8 in the Supplement.

## 2.4 Data analysis

The experimental IR spectra were analyzed using the program MALT which simulates experimental  
140 FTIR spectra (Griffith, 1996) combined with non-linear least squares fitting to best-fit the calculated spectra to measured spectra (Griffith et al., 2012) [new reference]. The MALT program generates a simulated spectrum from initial estimates of the absorber concentrations and instrument parameters. The residual between the experimental and simulated spectra is reduced through iteration. Simulated line-shapes are generated using HITRAN absorption parameters (version 2008) (Rothman et al.,  
145 2009) convolved with an FTIR instrument function simulating the Bruker IFS 66v/S instrument. The InSb detector covers a spectral range from 1800–5000 cm<sup>-1</sup> and the MCT detector covers a

**Table 1.** Experimental setup. The experiment numbers are listed in column Exp., the detector in the column Detect., the heavy CH<sub>4</sub> isotopologue included in the experiments are listed in column [<sup>x</sup>CH<sub>3</sub>D], the mean measured temperatures in the photoreactor are listed in column *T*, the H<sub>2</sub>O-vapour concentrations at the start of the experiments (*t* = 0) as obtain from spectral fitting are listed in column [H<sub>2</sub>O]<sub>*t*=0</sub>, the mean O<sub>3</sub> concentration after refill (i.e. the “top”-values) as obtain from spectral fitting are listed in column [O<sub>3</sub>]<sub>top</sub>, the <sup>12</sup>CH<sub>4</sub>-concentrations at the start of the experiments (*t* = 0) as obtain from spectral fitting are listed in column [<sup>12</sup>CH<sub>4</sub>]<sub>*t*=0</sub>, and the heavy CH<sub>4</sub> concentrations at the start of the experiments (*t* = 0) as obtain from spectral fitting are listed in column [<sup>x</sup>CH<sub>3</sub>D]<sub>*t*=0</sub>. Note that for the experiment including CH<sub>3</sub>D, the value of initial concentration only refers to [<sup>12</sup>CH<sub>3</sub>D]<sub>*t*=0</sub>.

Exp.	Detect.	<sup>x</sup> CH <sub>3</sub> D	<i>T</i>	[H <sub>2</sub> O] <sub><i>t</i>=0</sub>	[O <sub>3</sub> ] <sub>top</sub>	[ <sup>12</sup> CH <sub>4</sub> ] <sub><i>t</i>=0</sub>	[ <sup>x</sup> CH <sub>3</sub> D] <sub><i>t</i>=0</sub>
			/K	/hPa	/hPa	/hPa	/hPa
1	MCT	CH <sub>3</sub> D	298.2 ± 1.2	7.1	— <sup>a</sup>	0.030	0.054
2	MCT	CH <sub>3</sub> D	297.6 ± 0.8	5.6	0.19	0.058	0.042
3	MCT	CH <sub>3</sub> D	277.2 ± 0.2	5.2	0.29	0.109	0.046
4	MCT	CH <sub>3</sub> D	277.0 ± 0.2	5.1	0.16	0.073	0.035
5	InSb	CH <sub>3</sub> D	284.5 ± 0.1	7.2	0.26	0.025	0.033
6	InSb	CH <sub>3</sub> D	291.1 ± 0.2	7.4	— <sup>a</sup>	0.052	0.050
7	InSb	CH <sub>3</sub> D	313.5 ± 1.3	7.1	0.17	0.025	0.029
8	InSb	CH <sub>3</sub> D	312.4 ± 0.9	4.3	— <sup>a</sup>	0.022	0.040
9	InSb	<sup>13</sup> CH <sub>3</sub> D	298.5 ± 0.1	5.1	— <sup>a</sup>	0.035	0.026
10	InSb	<sup>13</sup> CH <sub>3</sub> D	297.6 ± 0.6	6.4	0.13	0.025	0.033
11	InSb	<sup>13</sup> CH <sub>3</sub> D	276.8 ± 0.8	5.4	— <sup>a</sup>	0.024	0.024
12	InSb	<sup>13</sup> CH <sub>3</sub> D	277.2 ± 1.3	5.1	— <sup>a</sup>	0.022	0.030
13	InSb	<sup>13</sup> CH <sub>3</sub> D	287.4 ± 1.2	5.4	— <sup>a</sup>	0.021	0.028
14	InSb	<sup>13</sup> CH <sub>3</sub> D	287.4 ± 0.4	4.5	— <sup>a</sup>	0.016	0.029
15	InSb	<sup>13</sup> CH <sub>3</sub> D	314.4 ± 1.0	5.2	0.26	0.023	0.037
16	InSb	<sup>13</sup> CH <sub>3</sub> D	313.8 ± 0.8	8.3	0.17	0.025	0.035

<sup>a</sup>Spectra recorded during or after photolysis, [O<sub>3</sub>]<sub>top</sub> not available

spectral range from 400–5000 cm<sup>−1</sup>. The concentrations of <sup>12</sup>CH<sub>3</sub>D and <sup>13</sup>CH<sub>3</sub>D were calculated from spectral fits in the region 2140–2302 cm<sup>−1</sup>, see Fig. 1 and 2 [new figures]. Interference from H<sub>2</sub>O, CO<sub>2</sub>, and CO was eliminated by including simulated spectra obtained from the HITRAN database in the fit. As there is no HITRAN data available for <sup>13</sup>CH<sub>3</sub>D in this region, the cross sections from 2000–2400 cm<sup>−1</sup> for this isotopologue were estimated by shifting the spectrum of <sup>12</sup>CH<sub>3</sub>D, see Joelsson et al. (2014). Concentrations of <sup>12</sup>CH<sub>4</sub> were calculated from spectral fits in the region 2838–2997 cm<sup>−1</sup>. Interference from <sup>13</sup>CH<sub>3</sub>D was reduced by including temperature adjusted reference spectra in the fit, and interference from <sup>12</sup>CH<sub>3</sub>D, H<sub>2</sub>O, and H<sub>2</sub>CO was by including

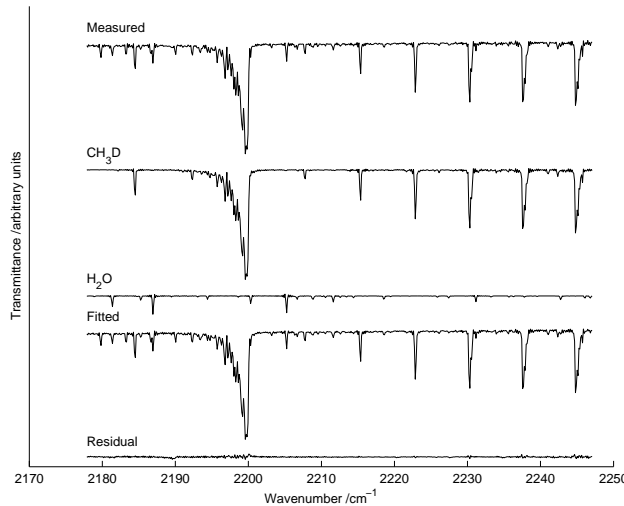


**Figure 1.** A typical spectral fit in the region where  $[^{12}\text{CH}_3\text{D}]$  is obtained (Experiment 5). Experimental data are shown by the topmost line, followed by the fitted (synthetic) partial spectra of the most dominant absorbers ( $\text{CH}_3\text{D}$  and  $\text{H}_2\text{O}$ ), the resulting fitted (synthetic) spectrum (also including  $\text{CO}_2$  and  $\text{CO}$ ), and the residual between the measured and fitted spectra is shown by the bottom line.

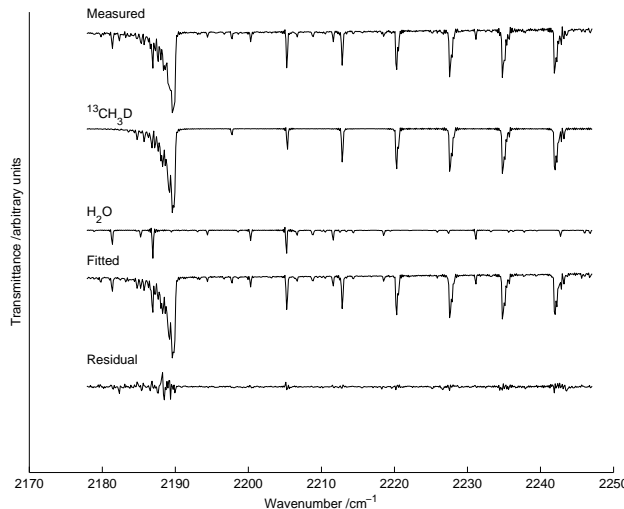


**Figure 2.** A typical spectral fit in the region where  $[^{13}\text{CH}_3\text{D}]$  is obtained (Experiment 10). Experimental data are shown by the topmost line, followed by the fitted (synthetic) partial spectra of the most dominant absorbers ( $^{13}\text{CH}_3\text{D}$  and  $\text{H}_2\text{O}$ ), the resulting fitted (synthetic) spectrum (also including  $\text{CO}_2$  and  $\text{CO}$ ), and the residual between the measured and fitted spectra is shown by the bottom line.

155 simulated spectra obtained from the HITRAN database in the fit, see Fig. 3 [new figure]. The spectral windows were sometimes adjusted to exclude saturated lines.

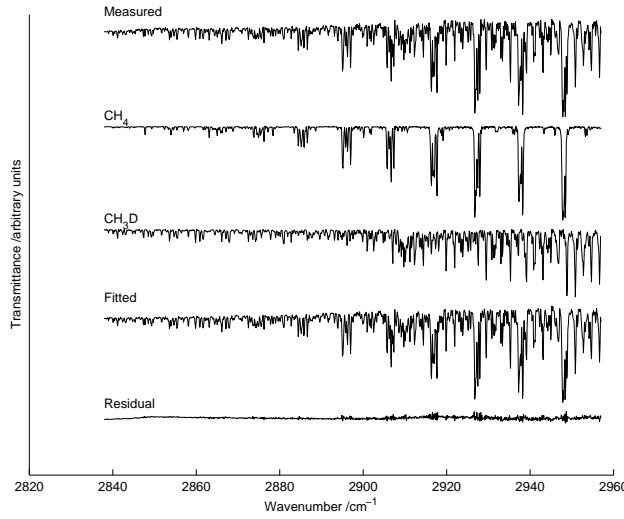


**Figure 3.** A typical spectral fit in the region where  $[^{12}\text{CH}_4]$  is obtained (Experiment 5). Experimental data are shown by the topmost line, followed by the fitted partial (synthetic) spectra of the most dominant absorbers ( $\text{CH}_4$  and  $\text{CH}_3\text{D}$ ), the resulting fitted (synthetic) spectrum (also including  $\text{H}_2\text{O}$ ), and the residual between the measured and fitted spectra is shown by the bottom line.

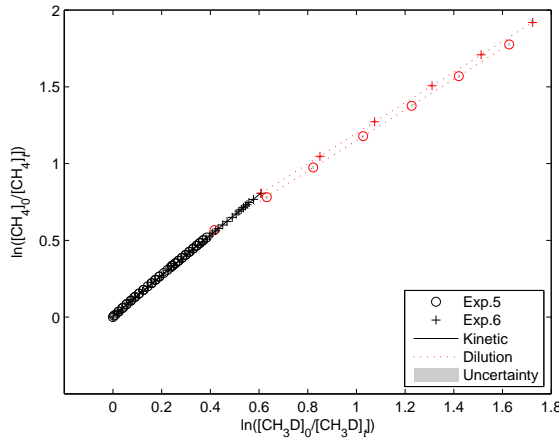


**Figure 4.** A typical experimental outcome, Experiment 5 and 6:  $\text{CH}_3\text{D}$ ,  $T = 288\text{K}$ . Experimental data are shown using black open circles (Exp. 5) and black plus signs (Exp. 6). Corresponding dilution test points are shown using red symbols. A linear fit of the experimental points is shown using a black solid line and linear fit of the subsequent dilution test are represented by a red dotted line, uncertainties for each point are represented by gray areas.

After  $[^x\text{CH}_3\text{D}]$  (where  $x = 12$  or  $x = 13$ ) and  $[^{12}\text{CH}_4]$  were obtained from the spectral analysis,  $\ln([^x\text{CH}_3\text{D}]_0/[^x\text{CH}_3\text{D}]_t)$  was plotted against  $\ln([^{12}\text{CH}_4]_0/[^{12}\text{CH}_4]_t)$  as described in Sect. 2.1. A straight line was fitted to these data points using a weighted total least squares routine (York et al.,

160 2004). The fitting procedure takes uncertainties in both dimensions into account. The uncertainty  $\sigma(\ln([A]_0/[A]_t))$  was calculated using standard error propagation:

$$\sigma(\ln([A]_0/[A]_t)) = \sqrt{\left(\frac{\sigma([A]_0)}{[A]_0}\right)^2 + \left(\frac{\sigma([A]_t)}{[A]_t}\right)^2} \quad (5)$$

where  $\sigma([A])$  was obtained as output from MALT. The fitting procedure, performed using a MATLAB script (York et al., 2004), also yields an error estimation which is defined as the uncertainty of the kinetic isotope effect  $\sigma(\alpha)$ . An example of a straight line fit can be found in Fig. 4 [new figure] and the full data set in Figs. S1–S8 in the Supplement. In the temperature dependence curve fitting procedure, the parameters  $A$  and  $B$  are from a linearized version of the Arrhenius equation:

$$\ln(k) = \ln(A) + B \cdot T^{-1} \quad (6)$$

are adjusted to match experimental. Also here, the method of York et al. (2004) was used. The 170 temperature in the cell was taken as the spatial average of the measurements from two thermocouples inside the temperature housing. The experiment temperature was defined by the temporal mean of the spatially averaged temperature measurement series and the uncertainty of the experiment temperature was the standard deviation of the spatially averaged temperature measurement series.

## 2.5 Kinetic model

175 A kinetic model was used to determine the influence of O(<sup>1</sup>D), reaction (R3), which rivals Reaction (R1). The model is previously described and was used by Nilsson et al. (2012). However, only the methane reaction subset and associated (O<sub>x</sub> and HO<sub>x</sub>) chemistry were used here. The Kintecus program (Ianni, 2003), simulates the photolysis of O<sub>3</sub> and the following oxidation chain of CH<sub>4</sub>. [sentence removed] To model ozone photolysis accurately, the modeled O<sub>3</sub> was matched to 180 the measured value by adjusting the photolysis rate, then the model was verified by comparing the decrease of CH<sub>4</sub> and the increase of H<sub>2</sub>O during the experiment. The model was run for each refill of O<sub>3</sub>, where the reaction rates of Reactions (R1) and (R3) were obtained. The model was designed for room temperature; experiments at other temperatures were not modeled. Experiment 2 was thus modeled: 4.4% of CH<sub>4</sub> was estimated to be lost to Reaction (R3). In an additional experiment N<sub>2</sub>O 185 was introduced in the chamber as an O(<sup>1</sup>D)-tracer. Since N<sub>2</sub>O does not react with OH and is not photolyzed at the wavelengths present (Nilsson et al., 2009), the decreased of N<sub>2</sub>O should be only due to Reaction (R8):



The amount of CH<sub>4</sub> lost by reaction (R3) can therefore be approximated by:

$$190 1 - \frac{[CH_4]_t}{[CH_4]_0} = 1 - \exp(-k_{(R3)}[O(^1D)]t) = 1 - \frac{[N_2O]_t}{[N_2O]_0}^{(k_{(R8)}/k_{(R3)})}, \quad (7)$$

where  $k_{(R8)} = 1.27 \times 10^{-10} \text{ cm}^{-3} \text{s}^{-1}$  and  $k_{(R3)} = 1.75 \times 10^{-10} \text{ cm}^{-3} \text{s}^{-1}$  (Sander et al., 2010). This gives 2.3% [CH<sub>4</sub>] lost by oxidation of O(<sup>1</sup>D), Reaction (R3). The kinetic model described above estimated that 4.7 % [CH<sub>4</sub>] were lost by Reaction (R3) **for this additional experiment**. Both methods agree that O(<sup>1</sup>D) loss is a minor channel. **No correction is applied, and the possible deviation is included in the estimated error.**

195 **included in the estimated error.**

### 3 Theoretical procedure

Rate constants and kinetic isotope effects for CH<sub>4</sub> + OH were calculated using a procedure similar to that employed by Joelsson et al. (2014).

#### 3.1 Computational chemistry calculations

200 The geometries of reactants, products and transition states were determined using a geometry optimization procedure based on the unrestricted MP2 method (Møller and Plesset, 1934) and the aug-cc-pVQZ orbital basis set (Dunning Jr., 1989; Woon and Dunning Jr., 1993). Harmonic vibrational frequencies for all relevant isotopologues of reactants, products, and transition states were obtained at the same level of theory. The calculations were carried out using the Gaussian 09 program package  
205 (Frisch et al., 2009).

The electronic energy of the optimized structures were refined using the CCSD(T) method (Watts et al., 1993; Knowles et al., 1993, 2000) with aug-cc-pVTZ, aug-cc-pVQZ, and aug-cc-pV5Z basis sets. The results from the different basis sets were used to extrapolate the electronic energy at the complete basis set limit following the approach of Halkier et al. (1998) as described by Joelsson  
210 et al. (2014).

#### 3.2 Rate constant calculations

The abstraction of a CH<sub>4</sub> hydrogen atom by OH can occur at four different sites. Depending on the methane isotopologue in question, these sites are either distinguishable or indistinguishable. Microscopic rate constants are calculated for hydrogen abstraction at each site using classical transition  
215 state theory with a tunneling correction factor,

$$k_{\text{micro}}^{(i)} = \eta_{\text{tun}}^{(i)} \frac{k_b T}{h} \frac{Q_{\text{TS}}^{(i)}}{Q_{\text{reac}}} \exp(-\Delta E^{(i)} / RT) \quad (8)$$

where  $\Delta E^{(i)}$  is the reaction barrier height (including the zero point vibrational energy) for the i'th reaction path.  $\eta_{\text{tun}}^{(i)}$  is a tunneling correction factor obtained using the Wigner tunneling correction (Wigner, 1932).  $Q_{\text{TS}}^{(i)}$  and  $Q_{\text{reac}}$  are the partition functions for the transition state and reacting pair,  
220 respectively. The total rate constant is obtained by summing over the microscopic rate constants.

**Table 2.** Results. The experiment numbers are listed in column Exp., the heavy CH<sub>4</sub> isotopologue included in the experiments are listed in column <sup>x</sup>CH<sub>3</sub>D, the mean measured temperatures in the photoreactor are listed in column *T*, the kinetic isotope effect corresponding to the isotopologue are listed in column  $\alpha$ , and the result of the dilution experiments are listed in column *k*<sub>dil</sub>.

Exp.	<sup>x</sup> CH <sub>3</sub> D	<i>T</i> /K	$\alpha$	<i>k</i> <sub>dil</sub>
1	CH <sub>3</sub> D	298.2 ± 1.2	1.302 ± 0.038	1.011 ± 0.048
2	CH <sub>3</sub> D	297.6 ± 0.8	1.314 ± 0.020	— <sup>a</sup>
3	CH <sub>3</sub> D	277.2 ± 0.2	1.294 ± 0.017	0.962 ± 0.037
4	CH <sub>3</sub> D	277.0 ± 0.2	1.335 ± 0.017	— <sup>a</sup>
5	CH <sub>3</sub> D	284.5 ± 0.1	1.334 ± 0.012	0.999 ± 0.009
6	CH <sub>3</sub> D	291.1 ± 0.2	1.323 ± 0.010	0.998 ± 0.010
7	CH <sub>3</sub> D	313.5 ± 1.3	1.301 ± 0.007	1.006 ± 0.031
8	CH <sub>3</sub> D	312.4 ± 0.9	1.338 ± 0.010	— <sup>a</sup>
9	<sup>13</sup> CH <sub>3</sub> D	298.5 ± 0.1	1.359 ± 0.022	1.000 ± 0.029
10	<sup>13</sup> CH <sub>3</sub> D	297.6 ± 0.6	1.314 ± 0.007	0.990 ± 0.064
11	<sup>13</sup> CH <sub>3</sub> D	276.8 ± 0.8	1.357 ± 0.046	1.016 ± 0.031
12	<sup>13</sup> CH <sub>3</sub> D	277.2 ± 1.3	1.344 ± 0.013	1.008 ± 0.030
13	<sup>13</sup> CH <sub>3</sub> D	287.4 ± 1.2	1.346 ± 0.025	1.009 ± 0.022
14	<sup>13</sup> CH <sub>3</sub> D	287.4 ± 0.4	1.342 ± 0.015	1.011 ± 0.019
15	<sup>13</sup> CH <sub>3</sub> D	314.4 ± 1.0	1.316 ± 0.016	1.003 ± 0.038
16	<sup>13</sup> CH <sub>3</sub> D	313.8 ± 0.8	1.331 ± 0.033	1.001 ± 0.034

<sup>a</sup>No dilution test performed

#### 4 Results and Discussion

The results of the 16 individual experiments (eight for each isotopologue) are tabulated in Table 2 [new table]. The resulting <sup>D</sup> $\alpha$ , <sup>13C</sup> $\alpha$ , and <sup>13C,D</sup> $\alpha$  values from the experimental and theoretical studies are tabulated in Tables 3, 4, and 5 [tables reordered] along with previous experimental and 225 theoretical results. The results are also shown in Fig. 5 and 6 for reactions of CH<sub>3</sub>D and <sup>13</sup>CH<sub>3</sub>D respectively.

The exponential curve fits yielded the parameters presented in Tables 3 and 5 giving <sup>D</sup> $\alpha_{\text{Arr}} = 1.32 \pm 0.13$  and <sup>13C,D</sup> $\alpha_{\text{Arr}} = 1.32 \pm 0.20$  at *T* = 298K. The mean of results of room temperature experiments Experiments 1 and 2, and Experiments 9 and 10 is <sup>D</sup> $\alpha_{\text{exp}} = 1.31 \pm 0.01$  and <sup>13C,D</sup> $\alpha_{\text{exp}} = 230$   $1.34 \pm 0.03$  [uncertainty corrected] respectively. It follows that  $\gamma_{\text{exp}} = 1.02 \pm 0.02$  at *T* = 298K, using <sup>13C</sup> $\alpha_{\text{exp}} = 1.0039 \pm 0.0002$  (Saueressig et al., 2001), meaning that the clumped isotope might react slower relative to what would be predicted based on the kinetic isotope effects of CH<sub>3</sub>D and <sup>13</sup>CH<sub>4</sub>. However, if the Arrhenius parameters are used to calculate the kinetic isotope effects at

**Table 3.** Experimental and theoretical studies of  $D\alpha$ . The temperature dependence studies are presented in the Arrhenius form  $D\alpha(T) = A(T/298K)^n \exp(BT^{-1})$ , where  $A$ ,  $n$ , and  $B$  are tabulated,  $T$  is the given temperature range, and  $D\alpha(T = 298K)$  is the resulting kinetic isotope effect at  $T = 298K$ . Where no  $B$  coefficient is presented  $A$  can be taken as  $D\alpha(T)$  for the given temperature range. All uncertainties are given as one standard deviation ( $\sigma$ ).

Study	$A$	$n$	$B/K$	$T/K$	$D\alpha(T = 298K)$
Experimental studies					
Present study <sup>a</sup>	$1.23 \pm 0.08$	0	$21 \pm 21$	[278,313]	$1.31 \pm 0.01^h$
Saueressig et al. (2001) <sup>b</sup>	$1.294 \pm 0.009$	–	–	296	–
Gierczak et al. (1997) <sup>c</sup>	$1.09 \pm 0.05$	0	$49 \pm 11$	[220,415]	$1.25 \pm 0.07$
DeMore (1993) <sup>a</sup>	0.91	0	75	[298,360]	1.17
Gordon and Mulac (1975) <sup>d</sup>	1.50	–	–	416	–
Gordon and Mulac (1975) <sup>d,i</sup>	1.06	–	–	416	–
Theoretical studies					
Present study <sup>e</sup>	1.314	0	6.354	[200,300]	1.339
Sellevåg et al. (2006) <sup>f</sup>	[1.30, 1.00]	–	–	[200,1500]	1.27
Masgrau et al. (2001) <sup>g,j</sup>	1.00	-0.02	50.5	[200,1500]	1.25

<sup>a</sup>Fourier transform infrared spectroscopy - relative rate

<sup>b</sup>Tunable diode laser absorption spectroscopy - isotope ratio mass sectrometer

<sup>c</sup>Pulsed photolysis - pulsed laser-induced fluorescence

<sup>d</sup>Pulse radiolysis

<sup>e</sup>Transition state theory with Wigner tunneling correction

<sup>f</sup>Canonical unified statistical theory

<sup>g</sup>Multicoefficient correlation method

<sup>h</sup>Average room temperature value, not obtained from curve fit

<sup>i</sup>Re-evaluated by DeMore (1993)

<sup>j</sup>Arrhenius parameters available at (NIST, 2015)

$T = 298K$ ,  $\gamma_{\text{Arr}} = 1.00 \pm 0.18$  (i.e. the reaction has no clumping effect). All uncertainties are given  
235 as one standard deviation ( $\sigma$ ). The theoretical results gives  $\gamma_{\text{theory}} = 1.00$  at  $T = 298K$ .

The present experimental room temperature results for  $D\alpha$  agree, to within the error bars, with the previous experimental studies, with the exception of DeMore (1993). DeMore (1993) used FTIR spectroscopy with a slow flow setup where the two methane isotopologues were measured separately with a common reference compound. The low  $D\alpha$  value in DeMore (1993) may be explained by  
240 interference from O(<sup>1</sup>D) radicals: OH radicals were produced by photolysis of O<sub>3</sub> at 254 nm in the presence of H<sub>2</sub>O, as in the present study. A relatively high rate of reaction (R3) would reduce the final kinetic isotope effect, since the kinetic isotope effect for oxidation with O(<sup>1</sup>D) is smaller than the kinetic isotope effect for the oxidation of OH (Saueressig et al., 2001). The present experimental results of  $D\alpha$  are also in good agreement with Masgrau et al. (2001) and Sellevåg et al. (2006). The

**Table 4.** Experimental and theoretical studies of  $^{13}\text{C}\alpha$ . The temperature dependence studies are presented in the Arrhenius form  $^{13}\text{C}\alpha(T) = A \exp(BT^{-1})$ , where  $A$  and  $B$  are tabulated,  $T$  is the given temperature range, and  $^{13}\text{C}\alpha(T = 298\text{K})$  is the resulting kinetic isotope effect at  $T = 298\text{K}$ . Where no  $B$  coefficient is presented  $A$  can be taken as  $^{13}\text{C}\alpha(T)$  for the given temperature range. All uncertainties are given as one standard deviation ( $\sigma$ ).

Study	$A$	$B/\text{K}$	$T/\text{K}$	$^{\text{D}}\alpha(T = 298\text{K})$
Experimental studies				
Saueressig et al. (2001) <sup>a</sup>	$1.0039 \pm 0.0002$	–	296	–
Cantrell et al. (1990) <sup>b</sup>	$1.0054 \pm 0.0005$	–	[273, 353]	$1.0054 \pm 0.0005$
Rust and Stevens (1980) <sup>c,i</sup>	1.003	–	–	–
Theoretical studies				
Present study <sup>d</sup>	1.0137	-1.219	[200,300]	1.0094
Sellevåg et al. (2006) <sup>e</sup>	[1.014, 1.00]	–	[200,1500]	1.003
Gupta et al. (1997) <sup>f</sup>	1.010	–	300	–
Melissas and Truhlar (1993) <sup>gh</sup>	[1.005, 1.001]	–	[223,416]	1.005
Lasaga and Gibbs (1991) <sup>h</sup>	[1.0036,1.0076]	–	[150,350]	–

<sup>a</sup>Tunable diode laser absorption spectroscopy - isotope ratio mass spectrometer

<sup>b</sup>Gas chromatography - mass spectrometry

<sup>c</sup>Isotope ratio mass spectrometry

<sup>d</sup>Transition state theory with Wigner tunneling correction

<sup>e</sup>Canonical variational transition state theory

<sup>f</sup>Conventional transition state theory

<sup>g</sup>Interpolated variational transition state theory with centrifugal-dominant, small-curvature tunneling coefficients

<sup>h</sup> Ab initio calculations

<sup>i</sup> No temperature information available

**Table 5.** Experimental and theoretical studies of  $^{13}\text{C},\text{D}\alpha$ . The temperature dependencies are presented in the Arrhenius form  $^{13}\text{C},\text{D}\alpha(T) = A \exp(BT^{-1})$ , where  $A$  and  $B$  are tabulated,  $T$  is the given temperature range, and  $^{13}\text{C},\text{D}\alpha(T = 298\text{K})$  is the resulting kinetic isotope effect at  $T = 298\text{K}$ . All uncertainties are given as one standard deviation ( $\sigma$ ).

Study	$A$	$B/\text{K}$	$T/\text{K}$	$^{\text{D}}\alpha(T = 298\text{K})$
Experimental study <sup>a</sup>	$1.18 \pm 0.10$	$38 \pm 26$	[278,313]	$1.34 \pm 0.03^c$
Theoretical study <sup>b</sup>	1.328	5.301	[200,300]	1.349

<sup>a</sup>Fourier transform infrared spectroscopy - relative rate

<sup>b</sup>Transition state theory with Wigner tunneling correction

<sup>c</sup>Average room temperature value, not obtained from curve fit

245 theoretical calculations of  $^{\text{D}}\alpha$  give a slightly higher value than the experimental results, although they are in good agreement with the best Arrhenius curve fit at  $T = 298\text{K}$ .

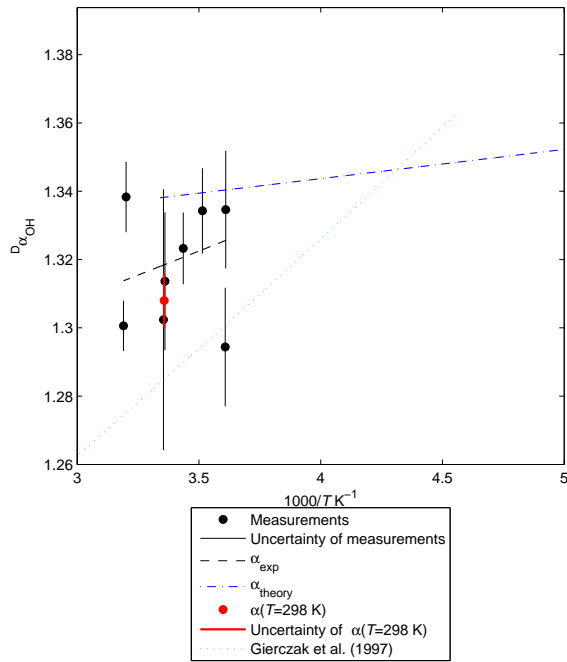


**Figure 5.** The individual measurements of  $D\alpha$ , are represented by black points; the accompanying individual error bars are represented by thin black solid lines; the experimental Arrhenius curve fit is represented by a black dashed line; the theoretical Arrhenius curve fit is represented by a blue dashed-dotted line; the mean of the room temperature measurements are represented by a red solid circle; the uncertainty of the room temperature measurements are represented by a thick red solid line; the result from Gierczak et al. (1997) (which is included for comparison) are represented by a green dotted line. All uncertainties are given as one standard deviation ( $\sigma$ ).

The experimental room temperature result for  $^{13}\text{C},D\alpha = 1.34 \pm 0.03$  agrees to within the error bar with both the theoretical value and the best estimate of the Arrhenius curve fit at  $T = 298\text{K}$ .

The theoretical calculations show a very small temperature dependence; the variability in the 250 experimental data is large compared to the value of the slope, making a quantification of the temperature dependence uncertain. Furthermore, the theoretical analysis revealed that the primary cause for the kinetic isotope effect is the substantially reduced reactivity of the D atom, which, in turn, can be explained by a significant increase in reaction barrier due to changes in vibrational zero point energy and to a lesser extent tunneling.

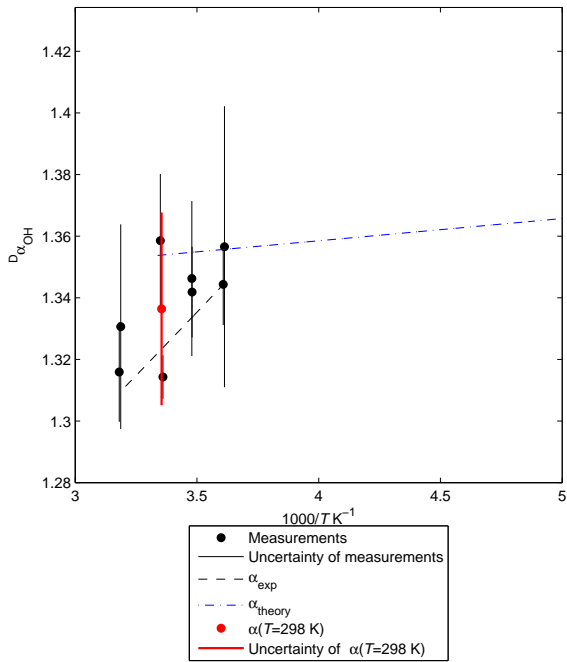


**Figure 6.** The individual measurements of  $^{13}\text{C},\text{D} \alpha$ , are represented by black points; the accompanying individual error bars are represented by thin black solid lines; the experimental Arrhenius curve fit is represented by a black dashed line; the theoretical Arrhenius curve fit is represented by a blue dashed-dotted line; the mean of the room temperature measurements are represented by a red solid circle; the uncertainty of the room temperature measurements are represented by a thick red solid line. All uncertainties are given as one standard deviation ( $\sigma$ ).

#### 255 4.1 Atmospheric implications

At steady state, assuming no clumping in emissions,  $\Delta(^{13}\text{CH}_3\text{D}) = \ln(\gamma)$ . It follows that  $\Delta(^{13}\text{CH}_3\text{D}) = 0.02 \pm 0.02$  implying that the clumped isotope effect of the OH reaction is very small. In turn, this implies that the bulk tropospheric  $\Delta(^{13}\text{CH}_3\text{D})$  reflects the source signal with relatively small adjustment due to the sink signal (i.e. mainly OH oxidation).  $\Delta(^{13}\text{CH}_3\text{D})$  would therefore be a more straightforward tracer for tracking methane sources than conventional isotopic analysis. However, the present uncertainty overrides the current estimated methane source signals (Wang et al., 2015), thus more precise measurements are necessary.

## 5 Conclusions

We present experimentally derived  $\text{CH}_4 + \text{OH}$  kinetic isotope effects and their temperature dependence for  $\text{CH}_3\text{D}$  and  $^{13}\text{CH}_3\text{D}$ ; the latter is reported for the first time. We find  ${}^{\text{D}}\alpha = 1.31 \pm 0.01$  and  ${}^{13}\text{C},{}^{\text{D}}\alpha = 1.34 \pm 0.03$  at room temperature, implying that the kinetic isotope effect is multiplicative such that  $(k_{\text{CH}_4}/k_{^{13}\text{CH}_4})(k_{\text{CH}_4}/k_{\text{CH}_3\text{D}}) = k_{\text{CH}_4}/k_{^{13}\text{CH}_3\text{D}}$  [new expression] to within the experimental uncertainty. We compare our experimental results to theoretical estimates derived using transition state theory with tunneling correction and kinetic isotope effects reported in the literature. We find good agreement between theoretical and literature values. Based on these experiments we find that the OH reaction (the main sink of methane) at steady-state has a clumped  $\Delta({}^{13}\text{CH}_3\text{D}) = 0.02 \pm 0.02$ .

*Acknowledgements.* This research has received funding from the European Community's Seventh Framework Programme (FP7/2007-2013) under grant agreement No. 237890, the Carlsberg foundation, and the Danish Council for Independent Research.

## References

- Allan, W., Lowe, D., and Cainey, J.: Active chlorine in the remote marine boundary layer: Modeling anomalous measurements of  $\delta^{13}\text{C}$  in methane, *Geophysical research letters*, 28, 3239–3242, 2001a.
- Allan, W., Manning, M., Lassey, K., Lowe, D., and Gomez, A.: Modeling the variation of  $\delta^{13}\text{C}$  in atmospheric methane: Phase ellipses and the kinetic isotope effect, *Global biogeochemical cycles*, 15, 467–481, 2001b.
- Bergamaschi, P., Bräunlich, M., Marik, T., and Brenninkmeijer, C. A.: Measurements of the carbon and hydrogen isotopes of atmospheric methane at Izaña, Tenerife: Seasonal cycles and synoptic-scale variations, *Journal of Geophysical Research: Atmospheres*, 105, 14 531–14 546, 2000.
- Cantrell, C., Shetter, R., McDaniel, A., Calvert, J., Davidson, J., Lowe, D., Tyler, S., Cicerone, R., and Greenberg, J.: Carbon Kinetic Isotope Effect in the Oxidation of Methane by the Hydroxyl Radical, *J. Geophys. Res.*, 95, 22 455–22 462, 1990.
- Ciais, P., Sabine, C., Bala, G., Bopp, L., Brovkin, V., Canadell, J., Chhabra, A., DeFries, R., Galloway, J., Heimann, M., Jones, C., Le Quéré, C., Myneni, R., Piao, S., and Thornton, P.: Carbon and Other Biogeochemical Cycles. In: Climate Change 2013: The Physical Science Basis. Contribution of Working Group I to the Fifth Assessment Report of the Intergovernmental Panel on Climate Change, Cambridge University Press, Cambridge, United Kingdom and New York, NY, USA, 2013.
- Crowley, J. N., Saueressig, G., Bergamaschi, P., Fischer, H., and Harris, G. W.: Carbon kinetic isotope effect in the reaction  $\text{CH}_4 + \text{Cl}$ : a relative rate study using FTIR spectroscopy, *Chem. Phys. Lett.*, 303, 268–274, 1999.
- DeMore, W.: Rate constant ratio for the reactions of OH with  $\text{CH}_3\text{D}$  and  $\text{CH}_4$ , *Journal of physical chemistry*, 97, 8564–8566, 1993.
- Dunning Jr., T. H.: Gaussian basis sets for use in correlated molecular calculations. I. The atoms boron through neon and hydrogen, *J. Chem. Phys.*, 90, 1007–1023, 1989.
- Eiler, J. M., Clog, M., Magyar, P., Piasecki, A., Sessions, A., Stolper, D., Deerberg, M., Schlueter, H. J., and Schwieters, J.: A high-resolution gas-source isotope ratio mass spectrometer, *International Journal of Mass Spectrometry*, 335, 45–56, 2013.
- Feilberg, K. L., Griffith, D. W. T., Johnson, M. S., and Nielsen, C. J.: The  $^{13}\text{C}$  and D kinetic isotope effects in the reaction of  $\text{CH}_4$  with Cl, *Int. J. Chem. Kinet.*, 37, 110–118, 2005.
- Ferretti, D. F., Miller, J. B., White, J. W. C., Etheridge, D. M., Lassey, K. R., Lowe, D. C., Meure, C. M. M., Dreier, M. F., Trudinger, C. M., van Ommen, T. D., and Langenfelds, R. L.: Unexpected changes to the global methane budget over the past 2000 years, *Science*, 309, 1714–1717, 2005.
- Frisch, M. J., Trucks, G. W., Schlegel, H. B., Scuseria, G. E., Robb, M. A., Cheeseman, J. R., Scalmani, G., Barone, V., Mennucci, B., Petersson, G. A., Nakatsuji, H., Caricato, M., Li, X., Hratchian, H. P., Izmaylov, A. F., Bloino, J., Zheng, G., Sonnenberg, J. L., Hada, M., Ehara, M., Toyota, K., Fukuda, R., Hasegawa, J., Ishida, M., Nakajima, T., Honda, Y., Kitao, O., Nakai, H., Vreven, T., Montgomery, Jr., J. A., Peralta, J. E., Ogliaro, F., Bearpark, M., Heyd, J. J., Brothers, E., Kudin, K. N., Staroverov, V. N., Kobayashi, R., Normand, J., Raghavachari, K., Rendell, A., Burant, J. C., Iyengar, S. S., Tomasi, J., Cossi, M., Rega, N., Millam, J. M., Klene, M., Knox, J. E., Cross, J. B., Bakken, V., Adamo, C., Jaramillo, J., Gomperts, R., Stratmann, R. E., Yazyev, O., Austin, A. J., Cammi, R., Pomelli, C., Ochterski, J. W., Martin, R. L., Morokuma, K., Zakrzewski, V. G., Voth, G. A., Salvador, P., Dannenberg, J. J., Dapprich, S., Daniels, A. D.,

- Farkas, O., Foresman, J. B., Ortiz, J. V., Cioslowski, J., and Fox, D. J.: Gaussian 09 Revision A.1, gaussian Inc. Wallingford CT 2009, 2009.
- Gierczak, T., Talukdar, R. K., Herndon, S. C., Vaghjiani, G. L., and Ravishankara, A. R.: Rate Coefficients for the Reactions of Hydroxyl Radicals with Methane and Deuterated Methanes, *J. Phys. Chem. A*, 101, 320 3125–3134, 1997.
- Gordon, S. and Mulac, W. A.: Reaction of OH(X2-PI) radical produced by pulse-radiolysis of water-vapor, *International Journal of Chemical Kinetics*, 1, 289–299, 1975.
- Griffith, D., Deutscher, N., Caldow, C., Kettlewell, G., Rigganbach, M., and Hammer, S.: A Fourier transform infrared trace gas analyser for atmospheric applications, *Atmospheric Measurement Techniques Discussions*, 325 5, 3717–3769, 2012.
- Griffith, D. W. T.: Synthetic Calibration and Quantitative Analysis of Gas-Phase FT-IR Spectra, *Appl. Spectrosc.*, 50, 59–70, 1996.
- Gupta, M. L., McGrath, M. P., Cicerone, R. J., Rowland, F. S., and Wolfsberg, M.: C-12/C-13 kinetic isotope effects in the reactions of CH<sub>4</sub> with OH and Cl, *Geophysical Research Letters*, 24, 2761–2764, 1997.
- 330 Halkier, A., T., H., Jørgensen, P., Klopper, W., Koch, H., Olsen, J., and Wilson, A. K.: Basis-set convergence in correlated calculations on Ne, N<sub>2</sub>, and H<sub>2</sub>O, *Chem. Phys. Lett.*, 286, 243 – 252, 1998.
- Ianni, J.: A Comparison of the Bader-Deuflhard and the Cash-Karp Runge-Kutta Integrators for the GRI-MECH 3.0 Model Base on the Chemical Kinetics Code Kintecus, 2003.
- IPCC: Climate Change 2013: The Physical Science Basis. Contribution of Working Group I to the Fifth Assessment Report of the Intergovernmental Panel on Climate Change, Cambridge University Press, Cambridge, 335 United Kingdom and New York, NY, USA, 2013.
- Joelsson, L. M. T., Forecast, R., Schmidt, J. A., Meusinger, C., Nilsson, E. J. K., Ono, S., and Johnson, M. S.: Relative rate study of the kinetic isotope effect in the (CH<sub>3</sub>D)-C-13 + Cl reaction, *Chemical Physics Letters*, 605, 152–157, 2014.
- 340 Kirschke, S., Bousquet, P., Ciais, P., Saunois, M., Canadell, J. G., Dlugokencky, E. J., Bergamaschi, P., Bergmann, D., Blake, D. R., Bruhwiler, L., et al.: Three decades of global methane sources and sinks, *Nature Geoscience*, 6, 813–823, 2013.
- Knowles, P. J., Hampel, C., and Werner, H.-J.: Coupled cluster theory for high spin, open shell reference wave functions, *J. Chem. Phys.*, 99, 5219–5227, 1993.
- 345 Knowles, P. J., Hampel, C., and Werner, H.-J.: Erratum: “Coupled cluster theory for high spin, open shell reference wave functions” [ *J. Chem. Phys.* 99, 5219 (1993)], *J. Chem. Phys.*, 112, 3106–3107, 2000.
- Lasaga, A. C. and Gibbs, G.: Ab initio studies of the kinetic isotope effect of the CH<sub>4</sub> + OH• atmospheric reaction, *Geophysical Research Letters*, 18, 1217–1220, 1991.
- 350 Lassey, K. R., Etheridge, D. M., Lowe, D. C., Smith, A. M., and Ferretti, D. F.: Centennial evolution of the atmospheric methane budget: what do the carbon isotopes tell us?, *Atmos. Chem. and Phys.*, 7, 2119–2139, 2007.
- Liu, Q. and Liu, Y.: Clumped-isotope signatures at equilibrium of CH 4, NH 3, H 2 O, H 2 S and SO 2, *Geochimica et Cosmochimica Acta*, 175, 252–270, 2016.

- Lowe, D. C., Manning, M. R., Brailsford, G. W., and Bromley, A. M.: The 1991-1992 atmospheric methane  
355 anomaly: Southern Hemisphere C-13 decrease and growth rate fluctuations, *Geophys. Res. Lett.*, 24, 857–  
860, 1997.
- Ma, Q., Wu, S., and Tang, Y.: Formation and abundance of doubly-substituted methane isotopologues ((CH<sub>3</sub>D)-C-13) in natural gas systems, *Geochim. Cosmochim. Acta*, 72, 5446–5456, 2008.
- Masgrau, L., Gonzalez-Lafont, A., and Lluch, J. M.: The reactions CH<sub>n</sub>D<sub>4-n</sub> + OH → P and  
360 CH<sub>4</sub> + OD → CH<sub>3</sub> + HOD as a test of current direct dynamics multicoefficient methods to determine variational transition state rate constants. II, *Journal of Chemical Physics*, 115, 4515–4526, 2001.
- Melissas, V. S. and Truhlar, D. G.: Deuterium and C-13 kinetic isotope effects for the reaction of OH with CH<sub>4</sub>, *Journal of Chemical Physics*, 99, 3542–3552, 1993.
- Møller, C. and Plesset, M. S.: Note on an Approximation Treatment for Many-Electron Systems, *Phys. Rev.*,  
365 46, 618–622, 1934.
- Nilsson, E. J. K., Eskebjerg, C., and Johnson, M. S.: A photochemical reactor for studies of atmospheric chemistry, *Atmospheric Environment*, 43, 3029–3033, 2009.
- Nilsson, E. J. K., Andersen, V. F., Nielsen, O. J., and Johnson, M. S.: Rate coefficients for the chemical reactions of CH<sub>2</sub>F<sub>2</sub>, CHClF<sub>2</sub>, CH<sub>2</sub>FCF<sub>3</sub> and CH<sub>3</sub>CCl<sub>3</sub> with O(<sup>1</sup>D) at 298 K, *Chemical Physics Letters*, 554, 27–32,  
370 2012.
- NIST: National Institute of Standards and Technology Chemical Kinetics Database, <http://kinetics.nist.gov>, last access: 2 October 2015, 2015.
- Ono, S., Wang, D. T., Gruen, D. S., Sherwood Lollar, B., Zahniser, M. S., McManus, B. J., and Nelson, D. D.: Measurement of a Doubly Substituted Methane Isotopologue, <sup>13</sup>CH<sub>3</sub>D, by Tunable Infrared Laser Direct  
375 Absorption Spectroscopy, *Analytical chemistry*, 86, 6487–6494, 2014.
- Pohlman, J., Kaneko, M., Heuer, V., Coffin, R., and Whiticar, M.: Methane sources and production in the northern Cascadia margin gas hydrate system, *Earth and Planetary Science Letters*, 287, 504–512, 2009.
- Quay, P., Stutsman, J., Wilbur, D., Snover, A., Dlugokencky, E., and Brown, T.: The isotopic composition of atmospheric methane, *Global Biogeochemical Cycles*, 13, 445–461, 1999.
- Rothman, L. S., Gordon, I. E., Barbe, A., Benner, Bernath, P. F., Birk, M., Boudon, V., Brown, L. R., Campargue, A., and Champion, J. P.: The HITRAN 2008 molecular spectroscopic database, *J. Quant. Spec. and Rad. Trans.*, 110, 533–572, 2009.
- Rust, F. and Stevens, C.: Carbon kinetic isotope effect in the oxidation of methane by hydroxyl, *International Journal of Chemical Kinetics*, 12, 371–377, 1980.
- Sander, S. P., Friedl, R., Barker, J., Golden, D., Kurylo, M., Moortgat, G., Wine, P., Abbatt, J., Burkholder, J., Kolb, C., Moortgat, G., Huie, R., VL, O., et al.: Chemical kinetics and photochemical data for use in atmospheric studies: evaluation number 17, National Aeronautics and Space Administration, Jet Propulsion Laboratory, California Institute of Technology Pasadena, CA, 2010.
- Saueressig, G., Bergamaschi, P., Crowley, J. N., Fischer, H., and Harris, G. W.: Carbon kinetic isotope effect in  
390 the reaction of CH<sub>4</sub> with Cl atoms, *Geophys. Res. Lett.*, 22, 1225–1228, 1995.
- Saueressig, G., Bergamaschi, P., Crowley, J. N., Fischer, H., and Harris, G. W.: D/H kinetic isotope effect in the reaction CH<sub>4</sub> + Cl, *Geophys. Res. Lett.*, 23, 3619–3622, 1996.

- Saueressig, G., Crowley, J. N., Bergamaschi, P., Bruhl, C., Brenninkmeijer, C. A. M., and Fischer, H.: Carbon 13 and D kinetic isotope effects in the reactions of CH<sub>4</sub> with O(D-1) and OH: New laboratory measurements  
395 and their implications for the isotopic composition of stratospheric methane, *J. Geophys. Res.-Atmos.*, 106, 23 127–23 138, 2001.
- Schmidt, J. A. and Johnson, M. S.: Clumped isotope perturbation in tropospheric nitrous oxide from stratospheric photolysis, *Geophysical Research Letters*, 42, 3546–3552, 2015.
- Schmidt, J. A., Johnson, M. S., and Schinke, R.: Carbon dioxide photolysis from 150 to 210 nm: Singlet and  
400 triplet channel dynamics, UV-spectrum, and isotope effects, *Proceedings of the National Academy of Sciences*, 110, 17 691–17 696, 2013.
- Sellevåg, S. R., Nyman, G., and Nielsen, C. J.: Study of the carbon-13 and deuterium kinetic isotope effects in the Cl and OH reactions of CH<sub>4</sub> and CH<sub>3</sub>Cl, *Journal of Physical Chemistry A*, 110, 141–152, 2006.
- Stolper, D. A., Sessions, A. L., Ferreira, A. A., Santos Neto, E. V., Schimmelmann, A., Shusta, S. S., Valentine,  
405 D. L., and Eiler, J. M.: Combined C-13-D and D-D clumping in methane: Methods and preliminary results, *Geochimica Et Cosmochimica Acta*, 126, 169–191, 2014.
- Tyler, S. C., Rice, A. L., and Ajie, H. O.: Stable isotope ratios in atmospheric CH<sub>4</sub>: Implications for seasonal sources and sinks, *J. Geophys. Res.-Atmos.*, 112, 2007.
- Wang, D. T., Gruen, D. S., Lollar, B. S., Hinrichs, K.-U., Stewart, L. C., Holden, J. F., Hristov, A. N., Pohlman,  
410 J. W., Morrill, P. L., Koenneke, M., Delwiche, K. B., Reeves, E. P., Sutcliffe, C. N., Ritter, D. J., Seewald, J. S., McIntosh, J. C., Hemond, H. F., Kubo, M. D., Cardace, D., Hoehler, T. M., and Ono, S.: Nonequilibrium clumped isotope signals in microbial methane, *Science*, 348, 428–431, 2015.
- Watts, J. D., Gauss, J., and Bartlett, R. J.: Coupled-cluster methods with noniterative triple excitations for restricted open-shell Hartree–Fock and other general single determinant reference functions. Energies and  
415 analytical gradients, *J. Chem. Phys.*, 98, 8718–8733, 1993.
- Wigner, E.: On the quantum correction for thermodynamic equilibrium, *Physical Review*, 40, 749, 1932.
- Woon, D. E. and Dunning Jr., T. H.: Gaussian basis sets for use in correlated molecular calculations. III. The atoms aluminum through argon, *J. Chem. Phys.*, 98, 1358–1371, 1993.
- York, D., Evensen, N. M., Martínez, M. L., and De Basable Delgado, J.: Unified equations for the slope, intercept, and standard errors of best straight line, *Am. J. Phys.*, 72, 367–375, 2004.  
420